JOURNAL OF SOLID STATE CHEMISTRY **139,** 52–56 (1998)
ARTICLE NO. SC987800

Ab Initio Structure Determination of New Rare Earth Fluoride Borates $Ln_3(BO_3)_2F_3$ (*Ln* = Sm, Eu, and Gd)

G. Corbel, R. Retoux, and M. Leblanc[1]

Laboratoire des Fluorures, UPRES-A 6010, Université du Maine, Avenue Olivier-Messiaen, 72085 Le Mans Cedex, France

Received September 22, 1997; in revised form February 16, 1998; accepted February 24, 1998

The crystal structures of $Ln_3(BO_3)_2F_3$ (*Ln* = Sm, Eu, and Gd) are determined *ab initio* from X-ray powder data. The unit cell is monoclinic, space group *C*2/*c*, $Z = 4$, with $a = 12.534(1)$ Å, $b = 6.237(1)$ Å, $c = 8.360(1)$ Å, $\beta = 97.404(6)^\circ$, $V = 648.1(2)$ Å^3 for $Gd_3(BO_3)_2F_3$. The Rietveld refinement reliability converged to $R_p = 0.121$, $R_{wp} = 0.147$, $R_{exp} = 0.050$, $\chi^2 = 8.75$. The structure presents a 3D network of Archimedian monocapped antiprisms $Gd(1)O_4F_5$ and $Gd(2)O_7F_2$. These polyhedra form trimeric entities $Gd_3O_{12}F_9$, which build infinite layers parallel to the (010) plane. © 1998 Academic Press

INTRODUCTION

Borates β-BaB_2O_4 (BBO) (1) and LiB_3O_5 (LBO) (2), oxoborates $Ca_4GdO(BO_3)_3$ (GdCOB) (3), and fluoride borates $KBe_2BO_3F_2$ (KBBF) (4) and $BaCaBO_3F$ (5, 6) have a wide transparency range (7). This property led us to search for nonlinear optical (NLO) materials with the object of extending the transmission band toward the ultraviolet region. Therefore, rare earth fluoride borates were investigated to study luminescence and optical properties. This paper deals with the preparation and *ab initio* structure determination of $Ln_3(BO_3)_2F_3$ (*Ln* = Sm, Eu, and Gd).

EXPERIMENTAL

The synthesis of the title compounds was achieved by solid state reaction in a platinum tube. Good quality samples were obtained by heating a stoichiometric mixture of B_2O_3, Ln_2O_3, and LnF_3 as follows: 3 h at 700°C, 24 h at 850°C for $Gd_3(BO_3)_2F_3$ or 900°C for $Sm_3(BO_3)_2F_3$ and $Eu_3(BO_3)_2F_3$, and cooling at 0.1°C/min. The X-ray diffraction patterns show the presence, in addition to $Ln_3(BO_3)_2F_3$, of $LnBO_3$ (≈30 weight%), except for the samarium sample, in which the oxide fluoride $Sm_4O_3F_6$ coexists. A weight loss of 1–2%, corresponding to the departure of BF_3, HF or H_2O (due to water contamination of B_2O_3), is observed.

The X-ray diffraction patterns of the sieved powders were recorded on a Siemens D500 diffractometer (Table 1). The structure of $Gd_3(BO_3)_2F_3$ was determined using the programs FULLPROF (8), SHELX-76 (9), and SHELXS-86 (10). Structure projections were realized with the program Diamond (11).

The high resolution electron microscopy (HREM) and electron diffraction (ED) studies were performed on a 200 kV JEOL 2010 electron microscope (tilt ± 30°). Specimens were prepared by suspending in alcohol very thin crystals obtained from a thorough grinding of a powdered sample. A few droplets of the suspension were put on a carbon-coated holey film. The chemical composition of the deposited material was determined by energy dispersive X-ray analysis (EDX) with a Kevex EDX Spectrometer coupled to the microscope.

STRUCTURE DETERMINATION

ED studies were performed on $Gd_3(BO_3)_2F_3$ and the approximate cell parameters and reflection conditions were determined ($a \approx 12.0$ Å, $b \approx 6.1$ Å, $c \approx 8.3$ Å, and $\beta \approx 95^\circ$). This a/b ratio, close to 2, explains the failure of the automatic indexation programs TREOR (12) and DICVOL (13) to accomplish the cell determination. Reciprocal space analysis of several microcrystals reveals the systematic reflection conditions hkl: $h + k = 2n$ (Fig. 1), $h0l$: $l = 2n$. Extra $00l$ reflections with $l = 2n + 1$ were attributed to a double diffraction phenomenon (Fig. 1a, b^*c^* plane). The possible space groups are *C*2/*c* and *Cc*.

The EDX analysis indicates a fluorine : oxygen ratio close to 1 : 2. A pure oxygen compound, which appeared to be $GdBO_3$, was also found and was taken into account in the X-ray study.

The structure resolution was performed in the centric *C*2/*c* (No. 15) space group. The observed structure factors were extracted with FULLPROF in the "pattern matching" mode with a pseudoVoigt peak profile. The multisolution

[1] To whom correspondence should be addressed.

0022-4596/98 $25.00

TABLE 1
Conditions of X-ray Data Collection and Refinement for $Gd_3(BO_3)_2F_3$

Diffractometer, geometry	Siemens D500, Bragg-Brentano
Radiation	Cu$K\alpha$ (Graphite monochromator)
2θ range (°)	10–130
Step scan	0.02° (2θ)
Time per step	38 s
Slit aperture	0.15 mm
Space group	$C2/c$ (n°15)
Cell parameters (Å)	$a=12.534(1)$, $b=6.237(1)$, $c=8.360(1)$ $\beta=97.404(6)°$
Volume, Z	648.1(2) Å^3, 4
Number of reflections	553
Number of refined parameters	41
Zero point	0.134(1)° (2θ)
η (pseudoVoigt)	0.45(1)
Halfwidth parameters (U,V,W)	0.068(5), −0.033(5), 0.037(1)
Asymmetry parameters	0.129(4), 0.043(2)
Reliability factors	
Points with Bragg contribution	$R_p=0.121$, $R_{wp}=0.147$, $R_{exp}=0.050$, $\chi^2=8.75$
Structure reliability factors	$RB=0.095$, $RF=0.062$

TABLE 2
Atomic Coordinates and Isotropic Temperature Factors in $Gd_3(BO_3)_2F_3$

Atom	Site	x	y	z	Biso [Å^2]
Gd(1)	4e	0	0.8890(5)	$\frac{1}{4}$	0.24(6)
Gd(2)	8f	0.1777(1)	0.3922(3)	0.1772(2)	0.08(3)
O(1)	8f	0.650(1)	0.587(3)	0.359(2)	1.0
O(2)	8f	0.854(1)	0.241(2)	0.875(2)	1.0
O(3)	8f	0.268(1)	0.0822(3)	0.077(2)	1.0
F(1)	8f	0.454(1)	0.332(2)	0.965(2)	1.3(4)
F(2)	4e	0	0.518(3)	$\frac{1}{4}$	2.3(6)
B	8f	0.812	0.918	0.480	0.5

tangent direct method of SHELXS-86 gave the positions of two heavy atoms in 4e and 8f crystallographic sites ($R = 0.30$). Oxygen and fluorine were located by successive Fourier difference syntheses (SHELX-76). Only the coordinates of oxygen and fluorine, distinguished from valence bond analysis, were refined (FULLPROF). The oxygen temperature factors were fixed to the same value. The boron atomic positions, located from the final Fourier difference, could not be refined due to the weak boron diffusion factor. Consequently, only approximate boron–oxygen distances are given in Table 3. Information on data collection and Rietveld refinement are presented in Table 1.

The observed and calculated patterns are shown in Fig. 2. The atomic coordinates and isotropic factors are reported in Table 2. The selected interatomic distances are listed in Table 3.

The cell parameters of isostructural $Sm_3(BO_3)_2F_3$ and $Eu_3(BO_3)_2F_3$, refined with the "pattern matching" mode of FULLPROF, are presented in Table 4. The evolution of the cell volumes is linear with R_i^3 (R_i = rare earth ionic radius).

CHARACTERIZATION

A high resolution study of $Gd_3(BO_3)_2F_3$ was undertaken. Unfortunately $Gd_3(BO_3)_2F_3$ was rapidly damaged under the electron beam. Amorphous domains (white arrows), which grow with the beam exposure time, can be observed in Fig. 3.

A good through-focus series could not be recorded and a high resolution study with image simulation was not permitted. Thus, interpretation of the observed contrasts

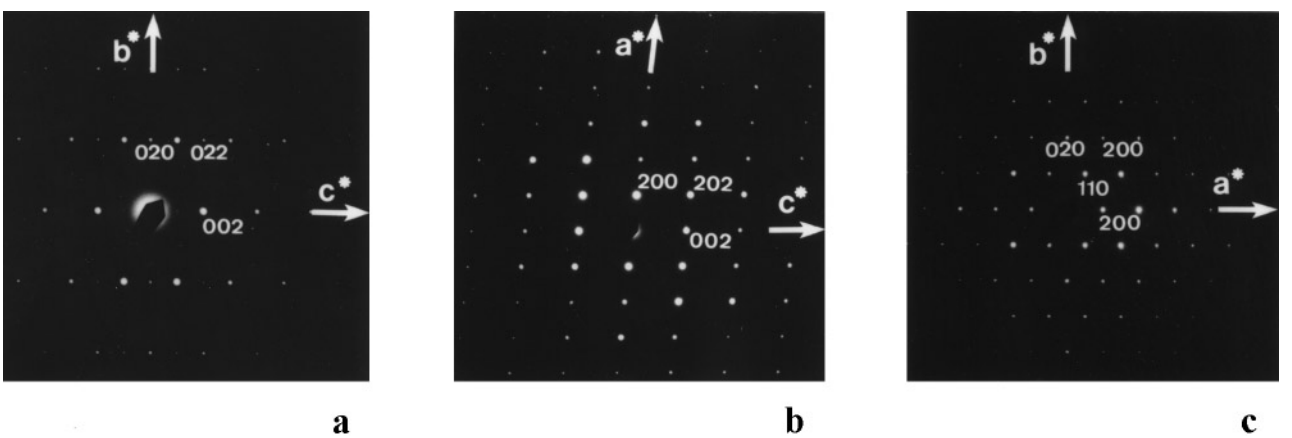

FIG. 1. [100], [010], and [001] ED patterns of $Gd_3(BO_3)_2F_3$.

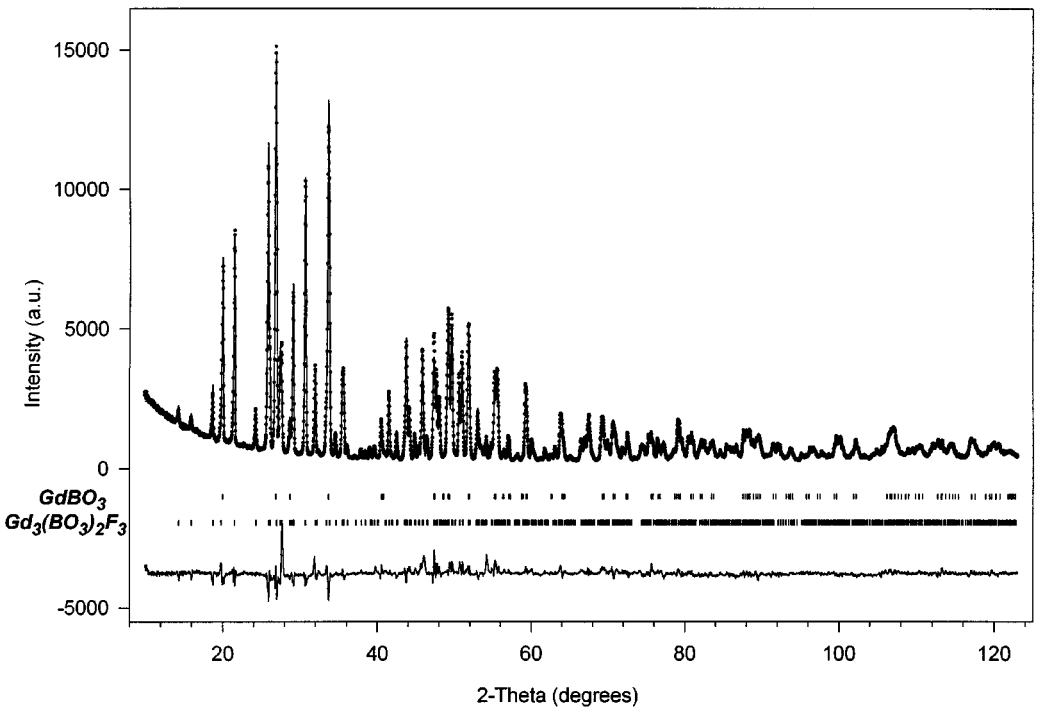

FIG. 2. Observed (dots) and calculated (line) X-ray powder diffraction diagrams. The difference pattern (observed − calculated) is shown at the bottom with the peak positions for $Gd_3(BO_3)_2F_3$ (lower) and $GdBO_3$ (upper).

TABLE 3
Selected Interatomic Distances (Å) and Angles (°) in $Gd_3(BO_3)_2F_3$

Gd(1) polyhedron			
1 × Gd–F(2)	2.32(2)	F(2)–Gd(1)–O(1)	122(1)
2 × Gd–O(1)	2.33(1)	O(1)–Gd(1)–O(1)	115.9(9)
2 × Gd–O(2)	2.37(2)	O(1)–Gd(1)–O(2)	129.5(9)
2 × Gd–F(1)	2.40(1)	O(2)–Gd(1)–O(2)	140.0(8)
2 × Gd–F(1)	2.62(1)	O(2)–Gd(1)–F(1)	106.7(8)
⟨Gd(1)–O,F⟩ = 2.42		F(1)–Gd(1)–F(1)	163(1)
		F(1)–Gd(1)–F(1)	137.2(5)
		F(1)–Gd(1)–F(1)	96.7(7)
Gd(2) polyhedron			
1 × Gd–O(3)	2.32(2)	O(3)–Gd(2)–O(2)	80(1)
1 × Gd–O(2)	2.35(1)	O(2)–Gd(2)–F(1)	113.0(8)
1 × Gd–F(1)	2.36(1)	F(1)–Gd(2)–O(3)	146.0(5)
1 × Gd–O(3)	2.39(1)	O(3)–Gd(2)–O(3)	126.4(6)
1 × Gd–O(3)	2.44(2)	O(3)–Gd(2)–O(1)	73(1)
1 × Gd–O(1)	2.49(2)	O(1)–Gd(2)–F(2)	83.7(9)
1 × Gd–F(2)	2.51(1)	F(2)–Gd(2)–O(1)	132.7(6)
1 × Gd–O(1)	2.54(2)	O(1)–Gd(2)–O(2)	65(1)
1 × Gd–O(2)	2.71(2)		
⟨Gd(2)–O,F⟩ = 2.46			
Borate BO_3^{3-} ion			
B–O(1)	1.37	O(1)–B–O(2)	117.6
B–O(2)	1.46	O(2)–B–O(3)	124.0
B–O(3)	1.47	O(3)–B–O(1)	118.4
⟨B–O⟩ = 1.43			

was not undertaken. Nevertheless, the images along the [100], [010] (Fig. 3), and [001] directions were recorded. The contrasts are regular and attest to good atomic ordering.

The characterization of $Gd_3(BO_3)_2F_3$ was performed by coupled TGA–DTA thermal analysis under argon (TA Instruments SDT 2960) (heating rate 10°C/min, temperature range 30–1475°C). A small continuous weight loss is observed above 500°C and decomposition of $Gd_3(BO_3)_2F_3$ occurs at 873°C. The resulting products are $GdBO_3$ and $Gd_4O_3F_6$.

STRUCTURE DESCRIPTION

A projection of the structure of $Gd_3(BO_3)_2F_3$ along [010] at $y \approx 0.25$ is given in Fig. 4. The structure can be described in terms of gadolinium polyhedra. Gadolinium atoms

TABLE 4
Cell Parameters of $Ln_3(BO_3)_2F_3$ (*Ln* = Sm, Eu, and Gd)

	a (Å)	*b* (Å)	*c* (Å)	*β* (°)	*V* (Å^3)	R_i^3 (Å)
$Sm_3(BO_3)_2F_3$	12.707(1)	6.2840(3)	8.4174(6)	97.306(6)	666.7(2)	1.450
$Eu_3(BO_3)_2F_3$	12.622(3)	6.271(1)	8.398(2)	97.278(9)	659.4(4)	1.405
$Gd_3(BO_3)_2F_3$	12.534(1)	6.237(1)	8.360(1)	97.404(6)	648.1(2)	1.356

FIG. 3. HREM image of the (010) plane of $Gd_3(BO_3)_2F_3$ (white arrows point out amorphous domains damaged under the electron beam).

occupy the centers of distorted $Gd(1)O_4F_5$ or $Gd(2)O_7F_2$ Archimedian antiprisms, monocapped on square faces. The mean Gd–(O,F) distances are in good agreement with the sum of ionic radii of Gd^{3+} (1.107 Å) and O^{2-} (1.35 Å) or F^- (1.285 Å): 2.42 Å and 2.46 Å (14). These polyhedra build infinite layers at $y \approx 0.25$ and $y \approx 0.75$, which are related by the inversion center at the origin. The connection of two Gd(2) and one Gd(1) polyhedra by opposite oxygen atom edges form trimeric entities $Gd_3O_{12}F_9$ approximately parallel to the (010) plane. The $Gd_3O_{12}F_9$ blocks are connected by oxygen atom edges to four other blocks in the same plane.

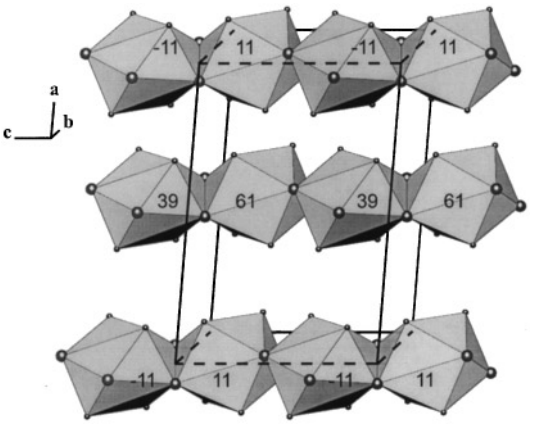

FIG. 5. Connection of the $Gd(1)O_4F_5$ polyhedra along [001]. The numbers indicate the coordinates of gadolinium atoms along *b* (in hundreds).

The $Gd(1)O_4F_5$ polyhedra are connected by fluorine atom edges to construct infinite isolated chains along the *c* axis (Fig. 5). Each Gd(1) polyhedron is connected to eight neighboring Gd(2) polyhedra and two Gd(1) polyhedra.

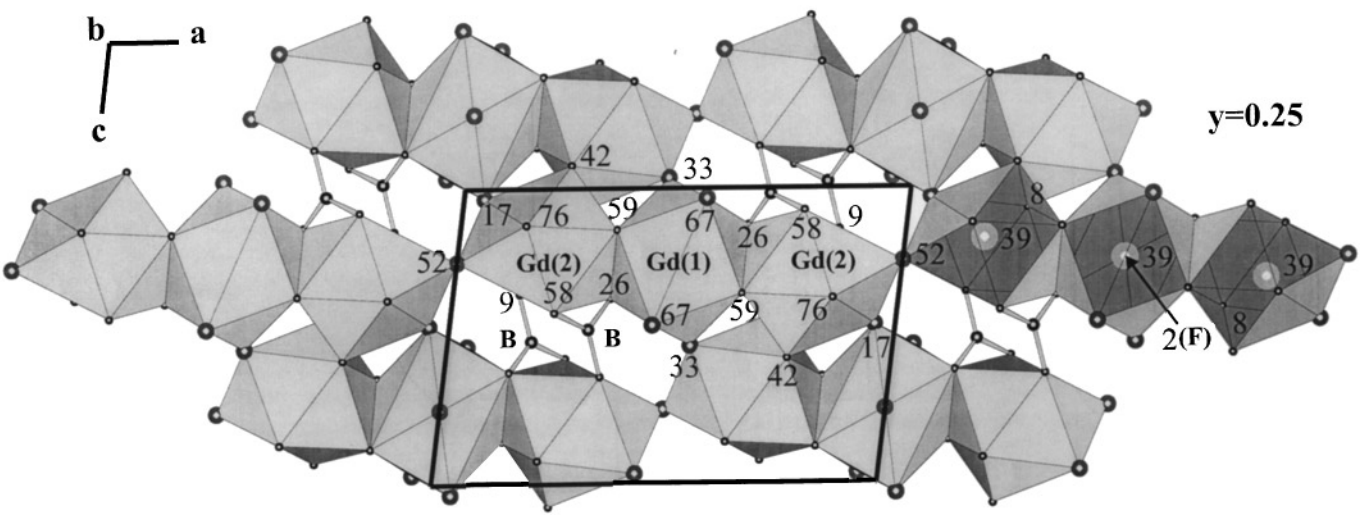

FIG. 4. [010] Projection of a layer of the structure $Gd_3(BO_3)_2F_3$ at $y \approx 0.25$ with gadolinium polyhedra and borate BO_3^{3-} ions. The front faces of three gadolinium polyhedra are opened. The numbers indicate the coordinates of atoms along *b* (in hundreds). Large circles represent fluorine atoms.

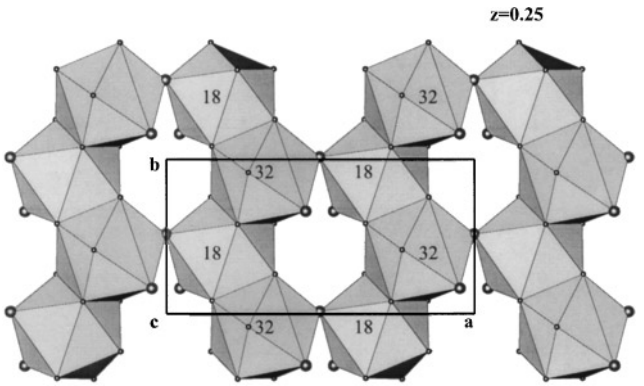

FIG. 6. Connection of the $Gd(2)O_7F_2$ polyhedra in the (001) plane at $z \approx 0.25$. The numbers indicate the coordinates of gadolinium atoms along c (in hundreds).

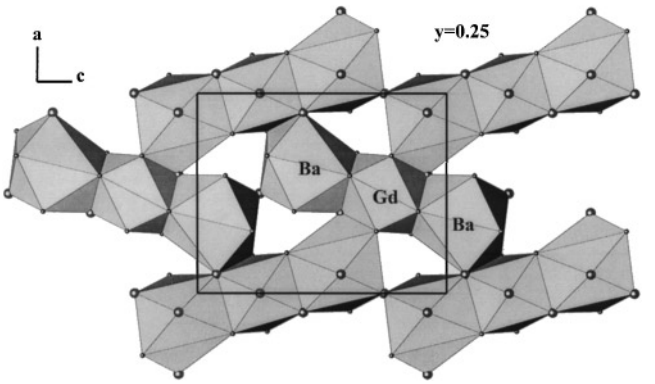

FIG. 7. Polyhedral arrangement in $Ba_2Gd(CO_3)_2F_3$.

The $Gd(2)O_7F_2$ polyhedra share triangular faces and form infinite chains parallel to the b axis at $z \approx 0.25$. These chains are joined by fluorine atoms in the (001) plane (Fig. 6) and by oxygen atoms along c. Consequently, the Gd(2) polyhedra build a 3D network in which the Gd(1) chains are inserted.

Each borate ion shares oxygen atom edges with one Gd(1) polyhedron and one Gd(2) polyhedron. The mean B–O distance, 1.43 Å, is close to that found generally in borates with a tricoordinated boron atom ($Ca_5(BO_3)_3F$: 1.38 Å (15); $NaBe_2BO_3F_2$ (NBBF): 1.37 Å (16); and $NdAl_3(BO_3)_4$ (NAB): 1.393 Å (17)). Grice *et al.* (18) have proposed a description of carbonate minerals based on the orientation of triangular CO_3^{2-} groups. From this, the arrangement of triangular borate groups can be described as layers, parallel to (001), of standing-on-edge BO_3^{3-} ions (Fig. 4).

It is interesting to note that similar trimeric entities $M_3O_{12}F_9$ (M = Ba, Gd) build the structure of the fluoride carbonate $Ba_2Gd(CO_3)_2F_3$ (19) (Fig. 7). This last phase and $Gd_3(BO_3)_2F_3$ result from the hypothetical substitution: $3Gd^{3+} + 2BO_3^{3-} \leftrightarrow 2Ba^{2+} + Gd^{3+} + 2CO_3^{2-}$. Barium and gadolinium atoms are also ninefold coordinated in $Ba_2Gd(CO_3)_2F_3$; the formulation of the polyhedra are BaO_5F_4 and GdO_3F_6. They also form infinite layers; however, the arrangement and connection of the trimers differ from those found in $Gd_3(BO_3)_2F_3$.

CONCLUSION

Evidence for a new structural family of rare earth fluoride borates $Ln_3(BO_3)_2F_3$ (Ln = Sm, Eu, and Gd) is presented. The synthesis is achieved by solid state reaction and the monoclinic structure is determined *ab initio*. A preliminary study of $Eu_3(BO_3)_2F_3$ shows that the luminescence emission lines are broad and intense, particularly the $^5D_0 \rightarrow {}^7F_0$, $^7F_1 \rightarrow {}^7F_2$, and $^7F_1 \rightarrow {}^7F_4$ transitions (20). A multisite environment of Eu^{3+}, with a low symmetry, is also found and is consistent with the structure determination. However, further investigation of the selective excitation spectra is needed before publication of the luminescence results.

REFERENCES

1. C. Chen, B. Wu, A. Jiang, and G. You, *Scientia Sinica B* **28,** 235 (1985).
2. C. Chen, Y. Wu, A. Jiang, B. Wu, G. You, R. Li, and S. Lin, *J. Opt. Soc. Am. B* **6,** 616 (1989).
3. G. Aka, A. Kahn-Harari, D. Vivien, J.-M. Benitez, F. Salin and J. Godard, *Eur. J. Solid State Inorg. Chem.* **33,** 727 (1996).
4. L. P. Solov'eva and V. V. Bakakin, *Kristallografiya* **15,** 922 (1970).
5. D. A. Keszler, A. Akella, K. I. Schaffers, and T. Alekel, *in* "MRS Symposium Proceedings, New Materials for Advanced Solid-State Lasers" (B. H. T. Chai, Ed.) Vol. 329, p. 15, 1994.
6. K. I. Schaffers, L. D. Deloach, and S. A. Payne, *IEEE J. Quantum Electron.* **32**(5), 741 (1996).
7. V. G. Dmitriev, G. G. Gurzadyan, and D. N. Nikogosyan, "Handbook of Non-Linear Optical Crystals," Series in Optical Science, Vol. 64. Springer-Verlag, Berlin/New York, 1991.
8. J. Rodriguez-Carnajal, "Abstracts of the Satellite Meeting on Powder Diffraction of the XVth Congress of the IUCr," p. 127. Toulouse, France, 1990.
9 G. M. Sheldrick, "SHELX-76: Program for Crystal Structure Determination." Cambridge University Press, Cambridge, 1976.
10. G. M. Sheldrick, *in* "Crystallographic Computing 3" (G. M. Sheldrick, C. Krüger, and R. Goddard, Eds.) p. 175. Oxford University Press, Oxford, 1985.
11. G. Bergerhoff, "Diamond: Visual Crystal Structure Information System." Gerhard-Domagk-Str.1, 53121 Bonn, Germany, 1996.
12. P.-E. Werner, L. Eriksson, and J. Westdahl, *J. Appl. Crystallogr.* **18,** 367 (1985).
13. A. Boultif and D. Louër, *J. Appl. Crystallogr.* **24,** 987 (1991).
14. R. D. Shannon, *Acta Crystallogr. Sect A* **32,** 751 (1976).
15. L. Shirong, H. Qingzhen, Z. Yifan, J. Aidong, and C. Chuangtian, *Acta Crystallogr. Sect C* **45,** 1861 (1989).
16. L. Mei, Y. Wang, and C. Chen, *Mater. Res. Bull.* **29,** 81 (1994).
17. H. Y.-P. Hong and K. Dwight, *Mater. Res. Bull.* **9,** 1661 (1974).
18. J. D. Grice, J. Van Velthuizen, and R. A. Gault, *Can. Mineral.* **32,** 405 (1994).
19. N. Mercier and M. Leblanc, *Eur. J. Solid State Inorg. Chem.* **28,** 727 (1991).
20. E. Antic-Fidancev and M. Lemaitre-Blaise, personal communication.